Superlattices and Microstructures 52 (2012) 84–91

Contents lists available at SciVerse ScienceDirect

Superlattices and Microstructures

journal homepage: www.elsevier.com/locate/superlattices

Enhancement of optical properties and donor-related emissions in Y-doped ZnO

Ming Gao [a,b,c], Jinghai Yang [c,*], Lili Yang [c], Yongjun Zhang [c], Jihui Lang [c], Huilian Liu [c], Hougang Fan [c], Yunfei Sun [a,b,c], Zhiqiang Zhang [c], Hang Song [a]

[a] Key Laboratory of Excited State Processes, Changchun Institute of Optics, Fine Mechanics and Physics, Chinese Academy of Sciences, Changchun 130033, PR China
[b] Graduate School of the Chinese Academy of Sciences, Beijing 100049, PR China
[c] Key Laboratory of Functional Materials Physics and Chemistry of the Ministry of Education, Jilin Normal University, Siping 136000, PR China

ARTICLE INFO

Article history:
Received 25 February 2012
Accepted 17 March 2012
Available online 23 March 2012

Keywords:
Nanoparticles
Yttrium doping
Enhance UV emission

ABSTRACT

The $Zn_{1-x}Y_xO$ nanoparticles with good optical properties have been prepared by sol–gel method. The yttrium doping effect on the structures and optical properties were investigated by XRD, SEM, XPS and low temperature photoluminescence. The UV emission intensity of yttrium doped ZnO was over 300 times stronger than that of pure ZnO, which was an exciting result in enhancing the ultraviolet near band edge emission in photoluminescence from ZnO nanoparticles. The UV emission band of doped ZnO nanoparticles exhibits a red shift from 388 to 398 nm, indicating a shallow energy level near valence band has been formed due to the yttrium doping into ZnO lattices. The defect-related band is suppressed (I_D/I_{UV} = 1–0.83) considerably in $Zn_{1-x}Y_xO$ nanoparticles, revealing the quenching of the broad yellow-orange emission. The doping effect on the optical properties is investigated by temperature dependent photoluminescence. The experimental results indicated that the donor level of yttrium is deeper than that of undoped ZnO.

1. Introduction

Zinc oxide (ZnO) is a wide direct band gap semiconductor with band gap energy of 3.37 eV at room temperature [1–4]. Since it is an environmental friendly material, ZnO has been expected to be a new

* Corresponding author. Address: Institute of Condensed State Physics, Jilin Normal University, Siping 136000, PR China. Tel.: +86 434 3290009; fax: +86 434 3294566.
E-mail address: jhyanga1@jlnu.edu.cn (J. Yang).

0749-6036/$ - see front matter © 2012 Elsevier Ltd. All rights reserved.
http://dx.doi.org/10.1016/j.spmi.2012.03.016

attractive material for the potential applications in the fields of blue and ultra-violet light emitting and detectors [1,3,4]. To improve the optical properties of ZnO, different methods including varying fabrication conditions and post-treatment were tried to suppress defect emission and enhance UV emission [5–8]. For pure ZnO, usually, its native optical properties are not good enough for the high requirement in the practice applications. Fortunately, the embedded dopants in a single crystalline nanostructure would enable some novel physical properties come out, such as ferromagnetism, band gap renormalization, high conductivity, electron–phonon coupling effect, and catalytic activity modification [9,10]. Rare earth ions that have partially filled 4f shells, if incorporated into suitable matrixes, their intra-4f optical transitions become possible because of splitting induced by the crystal field of the matrix [7]. Although it is known that the ion radius of Y is close to that of Zn, the reports about yttrium doping effects are limited.

Photoluminescence (PL) spectroscopy is a powerful and nondestructive method to explore the optical characteristics of doped nanomaterials. Especially the low temperature PL can reveal the dissociation processes of the impurity bound excitons induced by the doping. So far, the low-temperature PL studies on rare-earth elements doped ZnO nanostructures are very rare [11,12]. Particularly, no report has been addressed on yttrium doped ZnO nanoparticles to the best of our knowledge.

In this paper, we have presented a comprehensive investigation of low temperature PL properties of yttrium doped ZnO nanoparticles grown by sol–gel method. The effects of yttrium doping on the optical properties of ZnO nanoparticles were also investigated in detail.

2. Experimental

Pure ZnO and yttrium-doped ZnO nanoparticles were prepared in this experiment. We have synthesized the yttrium-doped ZnO nanoparticles in the previous work [13]. But we carry out different growth conditions in order to prepare the optimized samples. The experimental details have been shown in the following. Zinc nitrate hexahydrate, citric acid and ethylene glycol were dissolved in distilled water while keeping at 3:1:1 M ratio. For pure ZnO nanoparticles, all reagents were analytical grade and no further purification was needed. The mixed solution was stirred for 2 h, and then kept in the drying cabinet for 18 h to form dried gel. The dried gel was kept in the box furnace at 400 °C for 1 h to get amorphous precursor of Zn–C–O composite powers. Then this precursor was sintered under 750 °C for 6 h. Finally, the white powders were obtained after cooling down to room temperature. For Y-doped ZnO nanoparticles, the yttrium nitrate hexahydrate was added into the above mentioned mixed solution and following the same drying process to get dried gel. The molar ratio of Y to Zn was 5%. The dried gel was sintering at 750 °C for 6 h to get $Zn_{1-x}Y_xO$ nanoparticles.

XRD (MAC Science, MXP18, Japan), SEM (Hitachi, S-570), Raman spectroscopy (514.5 nm, argon ion laser, Renishaw-inVia) and PL (325 nm, He–Cd Laser, Renishaw-inVia) were used to characterize the crystal structure, surface morphology and optical properties of ZnO nanoparticles.

3. Results and discussions

Fig. 1 shows XRD patterns of as-prepared ZnO and $Zn_{1-x}Y_xO$ nanoparticles. The diffraction peaks in the XRD spectra indicate that both samples have typical hexagonal wurtzite structures. No diffraction peaks of Y or other impurities phases are detected in our samples, indicating that Y ions would uniformly substitute into the Zn sites or interstitial sites in ZnO lattice. The valance state of Y ions in ZnO nanoparticles were examined by XPS spectrum as shown in the inset image of the Fig. 1. The peaks of $Y3d_{3/2}$ and $Y3d_{5/2}$ core levels are found to be centered at 159.5 ± 0.10 and 157.8 ± 0.10 eV, respectively. The peak positions depend on the local structure of the Y atoms, which provides the information about the chemical state. For Y_2O_3 the energy difference between $Y3d_{3/2}$ and $Y3d_{5/2}$ core levels is ~1.75 eV. In our case, the energy difference between them is ~1.70 eV, which gives the evidence that Y ions exhibit +3 valance state in $Zn_{1-x}Y_xO$ nanoparticles. Moreover, the major diffraction peaks shift slightly towards smaller diffraction angle compared to the as-prepared ZnO (a = 3.250 and c = 5.208) in the XRD patterns. The lattice parameter c calculated from the (002) peak of $Zn_{1-x}Y_xO$ nanoparticles is 5.223 nm. The increase of lattice constant suggested that the larger Y^{3+} substitutes

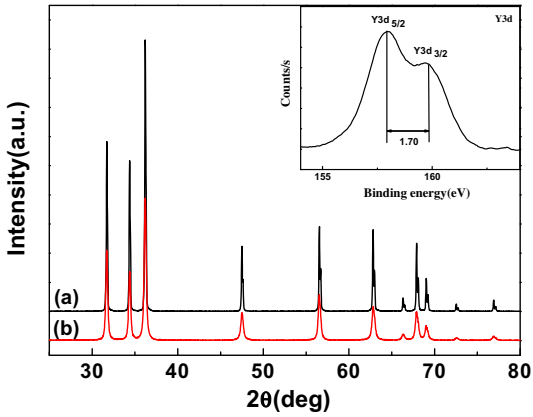

Fig. 1. XRD spectra of undoped ZnO (a) and Y-doped ZnO (b); the inset is the XPS spectra of Y 3d in Y-doped ZnO.

the smaller Zn^{2+} site partly so that the lattice constant increased. In addition, the peak intensity decreases and the width broaden, which implies that $Zn_{1-x}Y_xO$ nanoparticles with a smaller average diameter have been formed, which will be further proved by the SEM results below.

The morphology and microstructure of the as-grown materials are characterized and analyzed by SEM. SEM image (Fig. 2a) shows that the as-grown products prepared by sintering at 750 °C have a uniform size with the average diameter of about 100 nm. The yttrium doping ZnO nanoparticles with good quality can be obtained at the same temperature, the average diameter is ~20 nm in Fig. 2b, but exhibits a little aggregated.

Raman scattering is very sensitive to the microstructure of nanosized materials, which is expected in our case to obtain some useful information about the structure of yttrium doped ZnO nanoparticles. Fig. 3 shows the room-temperature Raman spectra of ZnO and yttrium doped ZnO excited by the 514.5 nm line of an argon laser, taken in the backscattering geometry. The zone-center optical phonons can be classified according to the following irreducible representations: $\Gamma_{opt} = A_1 + E_1 + 2E_2 + 2B_1$. The B_1 modes are silent modes, the A_1 and E_1 modes are polar modes and both Raman and infrared active, and they split into transverse optical (TO) and longitudinal optical (LO) phonons, whereas the E_2 modes are nonpolar and Raman active only. According to Fig. 3, the E_{2H} peak shows a dominant intensity and a very sharp feature,indicating that the wurtzite structure

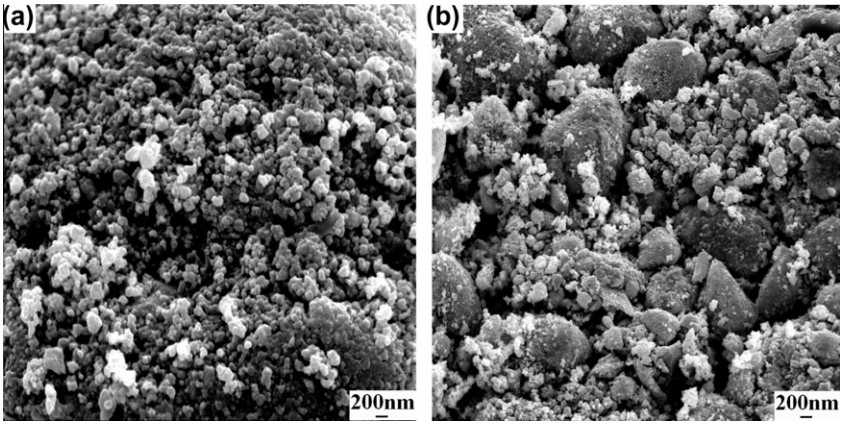

Fig. 2. SEM of undoped ZnO (a) and Y-doped ZnO (b).

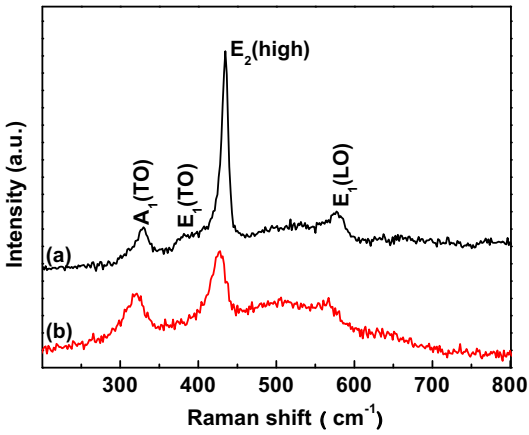

Fig. 3. Raman spectra of undoped ZnO (a) and Y-doped ZnO (b).

formed in pure ZnO and Y-doped ZnO with good crystal quality, which is in agreement with XRD result. Compared with pure ZnO nanoparticles, the peak position of E_{2H} modes in $Zn_{1-x}Y_xO$ nanoparticles blueshift from 434 to 431 cm^{-1}, and the intensities decrease. Usually, an increase in the E_{2H} phonon wavenumber is ascribed to compressive stress, whereas a decrease in the E_{2H} phonon wavenumber is ascribed to a tensile stress [14]. It is generally agreed that this stress arises from a mismatch in the thermal expansion coefficients of the nanoparticles, or the lattice mismatch and distortion. In our case, the yttrium doping is considered to be the main factor that would cause the lattice distortion of the crystals due to the ionic radius difference between Zn and Y ions. The E_{1L} peak centered at 580 cm^{-1} can be ascribed to the formation of the defects such as oxygen vacancy and Zn interstitial [15]. The Raman peak area ratio of the E_{2H} to the E_{1L} emission is 9 and 1.8, for ZnO and $Zn_{1-x}Y_xO$ nanoparticles, respectively. Generally, the peak area ratio of the E_{2H} to the E_{1L} emission is regarded as an indicator of the defects of ZnO materials. The decreased ratio further suggests the more lattice mismatch and distortion introduced by dopant.

The photoluminescence spectra of ZnO and yttrium-doped ZnO were measured with an excitation wavelength of 325 nm at room temperature, which consists of a UV peak at 398 nm in wavelength and a deep level emission (DLE) band in the range of 430–700 nm as shown in Fig. 4. The UV emission band

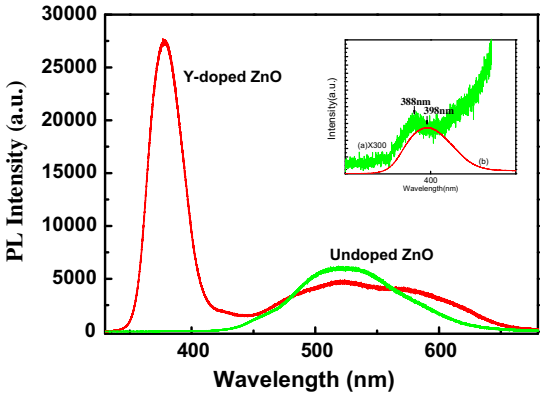

Fig. 4. Room temperature photoluminescence spectra of undoped ZnO (a), Y-doped ZnO (b); the inset is the compared the intensity increased 300 times of ZnO with yttrium doped ZnO in UV emission region.

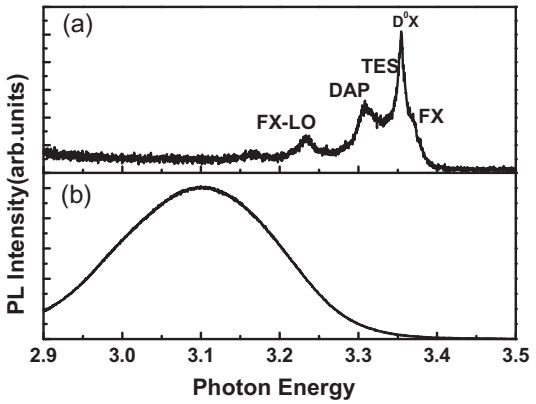

Fig. 5. Photoluminescence spectra of undoped ZnO (a) and Y-doped ZnO (b) measured at 79 K.

is related to a near band-edge transition of ZnO, namely, the recombination of the free excitons. The room temperature PL peak position can be different, for example the transition energy from 375 nm [16] to 383 nm [17], and the exact energy position depends on the contribution between the free exciton and the transition between free electrons to acceptor bound holes [18–21]. Recently, the DLE band in the green range had been identified and at least two different defect origins (V_O and V_{Zn}) with different optical characteristics were claimed to contribute to this band [22–24]. The deep level involved in the orange luminescence was attributed to the intrinsic defect in ZnO as zinc interstitials suggesting zinc excessive in the sample [25].

As shown in Fig. 4, the inset image clearly illustrated a 300 times enhancement of UV emission intensity for $Zn_{1-x}Y_xO$ nanoparticles compared to that of pure ZnO. Meanwhile, the emission intensity of DLE band is strongly suppressed after yttrium doping. Maybe the doped cations provide competitive pathways for recombination, which results in quenching of the broad yellow-orange emission. As discussed in the XPS results, Y^{3+} substituted the Zn^{2+} sites can reduce the Zn vacancies, leading to a decrease of the DLE band in the green region. As well as we known, under optical excitation, two competitive emission processes exist in the materials, one is UV emission and the other is DEL, but it unused in our experiment. In our case, on one hand, Y doping into the ZnO crystal lattice will reduce the quantity of nonradiative recombination centers, which will depress the nonradiative recombination. On the other hand, the intensity of DEL emission also decreases. That is to say, Y doping can suppress two kinds of defects and finally result in a stronger UV emission intensity in the PL spectra of $Zn_{1-x}Y_xO$ nanoparticles. In addition, as shown in the insert of Fig. 5, we can also observe the strong UV emission peak centering around 398 nm exhibits a red shift compared with that of pure ZnO 388 nm. The red shift could be ascribed to the defects and the probable shallow energy level caused by the incorporation of yittuim dopants into the ZnO lattices [26–28].

To better understand the intrinsic behavior, temperature-dependent PL measurements were performed. The low temperature (79 K) PL spectrums in the NBE region are plotted in Fig. 6. As shown in the Fig. 6a, for pure ZnO, the peaks at 3.375 and 3.230 eV are always attributed to the A-free exciton (FX) recombination and its second-order longitudinal optical (FX-2LO) phonon replica, respectively [29]. The energy separation of 145 meV has a good agreement with 2LO energy ($\hbar\omega_{LO} \approx 72$ meV). The sharp peak at 3.355 eV is due to neutral donor-bound exciton transition (D^0X) [30], originated from the intrinsic donor-like defects. The low-energy shoulder at 3.311 attributed to two-electron satellite (TES) transitions [31]. The D^0X and TES transitions, which correspond to an excited state of the donor, are very useful to determine the chemical identity of the donors. Therefore, the donor binding energy E_D in our case can be estimated from the equation $E_D = \frac{4}{3}(E_{D^0X} - E_{TES}) = 44$ meV, which is in good agreement with the reported value of 46.1 meV [32]. It is also interesting to note that the above donor binding energy follow quite well a linear proportionality to the bound exciton localization energy ($E_{FX} - E_{D^0X}$), which is called as Haynes rule. The calculated Haynes constant was 0.35, which well

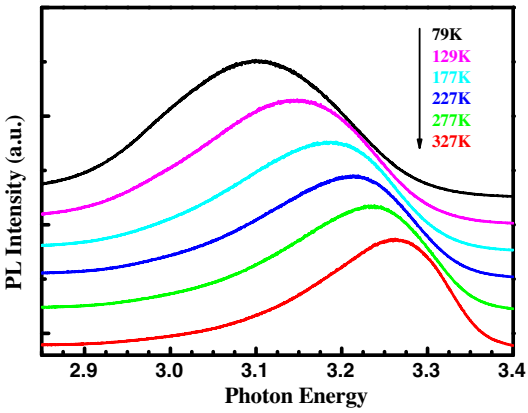

Fig. 6. Photoluminescence spectra of Y-doped ZnO measured from 79 to 327 K.

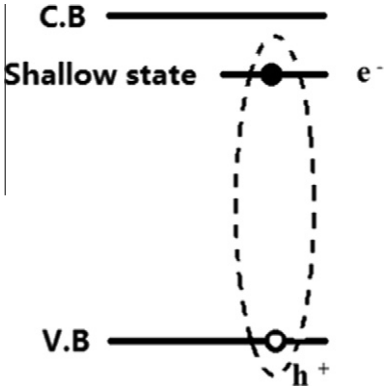

Fig. 7. Schematic showing the energy-band diagram of Y-doped ZnO. The conduction band (C.B), valance band (V.B).

agreed with the reported values 0.34 [33]. The above calculation results further proved that the assignment to the five photoluminescence peak was right.

Fig. 5b shows the experimental PL spectra of $Zn_{1-x}Y_xO$ measured at 79 K. The Y-doped ZnO is usually believed to contain large quantities of defects, most likely in the form of Zn and O vacancies and Y impurities. V_O would not form at the O-rich condition. After annealing, Y impurities substitutes for Zn sites and act as a donor. Since the UV peak position locates at 3.17 eV, we propose this emission is mainly caused by DAP recombination as reported in bulk ZnO [34] and similar to indium-doped ZnO [35]. In order to identify this peak is DAP, we performed the temperature dependent PL measurement, as show in Fig. 6. The donor concentration is increased inevitably via yttrium incorporation, which acts as a shallow donor in ZnO. With increasing temperature, the DAP lines redshifts slightly. As temperature further increase, the DAP line evolves in eA^0 transition, which locates at higher energy side of DAP line. This evolvement is a typical characteristic of the DAP line and a typical feature of thermal ionization of shallow donors via the pathway of $(D^0, A^0) \rightarrow D^0 + A^0 + e + h$. Due to the smaller binding energy of yttrium-related donor, the ionized free electrons in the conduction band prefer to recombine with the acceptors. In this case, the acceptor energy can also be estimated from the DAP emission by

$$E_A = E_g - E_D - E_{DAP} + \sqrt[3]{4\pi/3}(e^2/4\pi\varepsilon\varepsilon_0)N_{A,D}^{1/3},$$

where $N_{A,D}$ is the majority impurity concentration, $\varepsilon = 8.656$ is the specific dielectric constant and ε_0 is the dielectric constant in a vacuum. Making $N_{A,D}$ approximately equal to the hole density, and taking $E_D = 90$ meV [36,37], we can obtain the value of $E_A = 172$ meV.

An energy transfer model from the ZnO host to the Y^{3+} ion is presented in Fig. 7. In this model, the band tail (shallow state) formed near the bandgap plays an important role in the excitation of the Y^{3+} ions. When an excited electron is trapped in the shallow state, a hole is then attracted to the trap by the Coulomb interaction for formation of the electron–hole pair. This process permit excited carriers from producing excitonic recombination at the band edge, resulting in increase of excitonic emissions.

4. Conclusion

In summary, we have observed and characterized the optical activity of Y in Y-doped ZnO nanoparticles grown via sol–gel method. Optical properties of ZnO nanoparticles were significantly improved by yttrium doping. These results provide an experimental method to good modified photoluminescence properties of ZnO by the introduction of yttrium dopants, which is very important for both fundamental and applied points of view.

Acknowledgements

This work is supported by Program for the High Technology Research and Development of China (863) (No. 2009AA03Z303), Program for the National Natural Science Foundation of China (Grant No. 61008051), Program for the development of Science and Technology of Jilin province (Item Nos. 20082112, 20080151, 20090140 and 20100113), the Eleventh Five-Year Program for Science and Technology of Education Department of Jilin Province (Item No. 20090422 and 20100355), Program for the scientific research of Jilin Normal University (Item No. 2008051) and the Open Project Program of National Laboratory of Superhard Materials (Item No. 201004).

References

[1] Z.L. Wang, J. Phys.: Condens. Matter 16 (25) (2004) R829–R858.
[2] X. Wang, C.J. Summers, Z.L. Wang, NanoLetters 4 (3) (2004) 423–426.
[3] M.H. Huang, S. Mao, H. Feick, H.Q. Yan, Y.Y. Wu, H. Kind, E. Weber, R. Russo, P. Yang, Science 292 (5523) (2001) 1897–1899.
[4] C. Liu, J.A. Zapien, Y. Yao, X. Meng, C.S. Lee, S. Fan, Y. Lifshitz, S.T. Lee, Adv. Mater. 15 (10) (2003) 838–841.
[5] Y. Yang, B.K. Tay, X.W. Sun, J.Y. Sze, Z.J. Han, J.X. Wang, X.H. Zhang, Y.B. Li, S. Zhang, Appl. Phys. Lett. 91 (2007) (1923) 071921–071923.
[6] Y. Yang, X.W. Sun, B.K. Tay, Peter H.T. Cao, J.X. Wang, X.H. Zhang, J. Appl. Phys. 103 (2008) 064307–064311.
[7] Q. Zhao, X.Y. Xu, X.F. Song, X.Z. Zhang, D.P. Yu, C.P. Li, L. Guo, Appl. Phys. Lett. 88 (2006) 033102–033106.
[8] H.Q. Le, S. Tripathy, S.J. Chua, Appl. Phys. Lett. 92 (2008) (1913) 141910–141913.
[9] P.X. Gao, Z.L. Wang, J. Phys. Chem. B 106 (2002) 12653–12656.
[10] C. Ronning, P.X. Gao, Y. Ding, Z.L. Wang, Appl. Phys. Lett. 84 (2004) 783–787.
[11] Baochang. Cheng, Yanhe. Xiao, Wu. Guosheng, Lide. Zhang, Adv. Funct. Mater. 14 (2004) 913–919.
[12] Yoshikazu Terai, Kazuki Yoshida, M.H. Kamarudin, Yasufumi Fujiwara, Phys. Status Solidi C8 (2011) 519–521.
[13] Jinghai. Yang, Rui. Wang, Lili. Yang, Jihui. Lang, Maobin. Wei, Ming. Gao, Xiaoyan. Liu, Jian. Cao, Xue. Li, Nannan. Yang, J. Alloy. Compd. 509 (2011) 3606–3612.
[14] S.K. Sharma, G.J. Exarhos, Solid State Phenom. 55 (1997) 32–37.
[15] L.V. Azaroff, Introduction to Solids, McGraw-Hill, 1960 (pp. 371–372).
[16] Y. Chen, N.T. Tuan, Y. Segawa, H. Ko, S. Hong, T. Yao, Appl. Phys. Lett. 78 (2001) 1469–1472.
[17] W.I. Park, S.J. An, G.C. Yi, H.M. Jang, J. Mater. Res. 16 (2001) 1358–1362.
[18] B.P. Zhang, N.T. Binh, K. Wakatsuki, Y. Segawa, Y. Kashiwaba, K. Haga, Nanotechnology 15 (2004) S382.
[19] M.A.E.J.I.M.A. Keigou, U.E.D.A. Masaya, Shizuo FUJITA1 and Shigeo FUJITA, Jpn. J. Appl. Phys. 42 (2003) 2600–2603.
[20] Q.X. Zhao, M. Willander, R.E. Morjan, Q.H. Hu, E.E.B. Campbell, Appl. Phys. Lett. 83 (2003) 165–168.
[21] W.I. Park, Y.H. Jun, S.W. Jung, G.C. Yi, Appl. Phys. Lett. 82 (2003) 964–967.
[22] Q.X. Zhao, P. Klason, M. Willander, et al, Appl. Phys. Lett. 87 (2005) (1915) 211912–211915.
[23] T. Moe Børseth, B.G. Svensson, A.Yu. Kuznetsov, P. Klason, Q.X. Zhao, M. Willander, Appl. Phys. Lett. 89 (2006) 262112–262115.
[24] P. Klason, T.M. Børseth, Q.X. Zhao, et al, Solid State Commun. 145 (2008) 321–323.
[25] D. Li, Y.H. Leung, A.B. Djurisic, Z.T. Liu, M.H. Xie, S.L. Shi, S.J. Xu, W.K. Chan, Appl. Phys. Lett. 85 (2004) 1601–1602.
[26] X.H. Wang, D.X. Zhao, Y.C. Liu, J.Y. Zhang, Y.M. Lu, X.W. Fan, J. Cryst. Growth 263 (2004) 316–319.
[27] K. Vandheusen, W.L. Warren, C.H. Seager, D.R. Tallant, J.A. Voigt, B.N. Gnage, J. Appl. Phys. 79 (1996) 7983–7986.
[28] Y.R. Ryu, T.S. Lee, H.W. White, Appl. Phys. Lett. 83 (2003) 87–89.
[29] R. Kumar, N. Khare, V. Kumar, G.L. Bhalla, Appl. Surf. Sci. 254 (2008) 6509–6513.

[30] Y. Sun, G.M. Fuge, M.N.R. Ashfold, Chem. Phys. Lett. 396 (2004) 21–26.
[31] L. Wang, N.C. Giles, J. Appl. Phys. 94 (2003) 973–978.
[32] A. Teke, Ü. Özgür, S. Doğan, X. Gu, H. Morkoç, Phys. Rev. B 70 (2004) 195207–195210.
[33] S.A. Studenikin, N. Golego, M. Cocivera, J. Appl. Phys. 84 (1998) 2287–2290.
[34] B. Du Ahn, H.S. Kang, J.H. Kim, et al, J. Appl. Phys. 100 (2006) 093701–093704.
[35] J.G. Lu, L.P. Zhu, Z.Z. Ye, et al, J. Cryst. Growth 283 (2005) 413–416.
[36] Chao. Liu, Haiping. He, Luwei. Sun, Qian. Yang, Zhizhen. Ye, Lanlan. Chen, J. Appl. Phys. 109 (2011) 053507–053510.
[37] D.C. Look, Mater. Sci. Eng. B80 (2001) 383–388.